



CEBAF-TH-91-23

CEBAF

The Continuous Electron Beam Accelerator Facility
Theory Group Preprint Series

Additional copies are available from the authors.

The Southeastern Universities Research Association (SURA) operates the Continuous Electron Beam Accelerator Facility for the United States Department of Energy under contract DE-AC05-84ER40150

DISCLAIMER

This report was prepared as an account of work sponsored by the United States government. Neither the United States nor the United States Department of Energy, nor any of their employees, makes any warranty, express or implied, or assumes any legal liability or responsibility for the accuracy, completeness, or usefulness of any information, apparatus, product, or process disclosed, or represents that its use would not infringe privately owned rights. Reference herein to any specific commercial product, process, or service by trade name, mark, manufacturer, or otherwise, does not necessarily constitute or imply its endorsement, recommendation, or favoring by the United States government or any agency thereof. The views and opinions of authors expressed herein do not necessarily state or reflect those of the United States government or any agency thereof.

Factorization and Heavy Quark Symmetry in Hadronic B -meson Decays

Cathy Reader

Department of Physics, University of Toronto, Canada M5S 1A7

Nathan Isgur

Continuous Electron Beam Accelerator Facility, Newport News, Virginia 23606

Abstract

We discuss within the context of heavy quark symmetry a program for performing *model-independent* tests of the factorization scenario proposed by Dugan and Grinstein for hadronic B -meson decays. Preliminary, *model-dependent* results for decays to a D or D^* and one, two, or three pions are presented which indicate that the predictions of factorization are consistent with the present experimental situation. Our results suggest that such decays may not only provide a precision testing ground for factorization, but also an opportunity to study the properties of excited D mesons and to measure many of the universal form factors of heavy quark symmetry (including ones not otherwise readily accessible).

I. Introduction

Though analysis of hadronic weak decays of light hadrons is complicated, there is a long-standing belief that the corresponding decays of heavy hadrons may be simpler. This anticipated simplicity would arise if the current-current weak interaction were to factorize into a product of two single-current matrix elements. An early use of factorization was

made by Feynman [1] in 1964, who showed that $\Delta I = \frac{1}{2}$ weak hyperon decays were roughly consistent with this hypothesis, while those with $\Delta I = \frac{3}{2}$ were not. (See also the pioneering paper by Schwinger [1].) The use of factorization was pursued for $\Delta I = \frac{3}{2}$ decays of strangeness by many authors [2]. After the discovery of charm, factorization often formed the basis of attempts to explain D and D_s hadronic weak decays [3]. More recently, the phenomenology of the factorization hypothesis has been extensively developed for weak hadronic decays of charm and beauty by Bauer, Stech and Wirbel [4] and others [5].

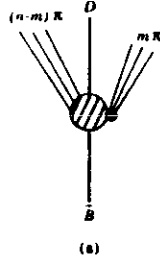
In parallel with this work have been several theoretical developments. Bjorken [6] has discussed a possible justification of factorization based on color transparency. Buras, Gerard and Rückl [7] have noted that factorization is valid as $1/N_c \rightarrow 0$ and have considered leading $1/N_c$ corrections to this limit. More recently, Dugan and Grinstein [8] have shown that, for \bar{B} and Λ_b decays, factorization follows from perturbative QCD in certain kinematic regions. They find that in the limit where m_b and m_c go to infinity with their ratio $r \equiv m_c/m_b$ fixed, matrix elements for processes like $\bar{B} \rightarrow D\pi^-$ and $\bar{B} \rightarrow D^*\pi^-$ factorize. Their argument depends on the large momentum (in the \bar{B} rest frame) of all the light quarks recoiling against the charmed system (in this case, those of the π^-), and is similar in spirit to the application of perturbative QCD to other exclusive processes. The major new feature is that in leading order the "hard exchange" is made by a four-quark operator rather than by a gluon. In this approach, hard gluon exchange gives small corrections of order α_s to factorization [9].

In this paper we will explain how the decays $\bar{B} \rightarrow D + n\pi$ and $\bar{B} \rightarrow D^* + (n-1)\pi$ may be used to make model-independent tests of Dugan-Grinstein factorization assuming the validity of the predictions of heavy quark symmetry [10,11] for heavy-meson weak form factors. We also discuss using such decays to measure some of the universal form factors of heavy quark symmetry which might otherwise be difficult to study. After introducing the framework for performing such model-independent tests, we present here, as a prelude to that more ambitious exercise, a preliminary model-dependent survey of the experimental situation which already indicates that the predictions of factorization and heavy quark symmetry are consistent with available data.

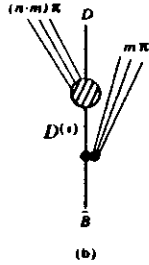
The basic program is a simple one. Roughly speaking, according to the factorization hypothesis, $\bar{B} \rightarrow D + n\pi$ proceeds when $\bar{B} \rightarrow D + (n-m)\pi$ via the $\bar{c}\gamma^\mu(1-\gamma_5)b$ current, while the current $\bar{d}\gamma^\mu(1-\gamma_5)u$ independently produces m pions (see Figure 1(a)). The former amplitude can be determined in terms of a few of the universal functions of heavy quark symmetry, while sufficient information about the latter process, up to $m\pi$ masses of m_τ , can be extracted from $\tau \rightarrow \nu_\tau + m\pi$ data. As we will indicate below, it is the region of low $m\pi$ mass where factorization is most likely to work, so the restriction to the mass region of the τ decay data is an appropriate one.

We have chosen to make an initial survey of the data in a model-dependent, resonance dominance framework (see Figs. 1(b) and 1(c)) for two reasons. First, it is simpler. At least as important, however, is our expectation that the $\bar{B} \rightarrow D + n\pi$ amplitudes will turn out to be dominated by resonant mechanisms involving $\bar{B} \rightarrow D^{(*)}$ transitions, where $D^{(*)}$ represents a charmed meson which can decay strongly to $D + (n-m)\pi$. Even if such resonances are not completely dominant, some will undoubtedly be sufficiently prominent that their production can be studied independently. In this case, these calculations will still be useful since the form factors for transitions to prominent resonances are themselves very interesting. As we will discuss below, if factorization holds, then for $D^{(*)}$'s other than the D and D^* , these form factors might be most easily measured in hadronic weak decays of the \bar{B} . Heavy-quark symmetry predicts all of the form factors for $\bar{B} \rightarrow D^{(*)}$ transitions in terms of a single [12] "universal function" for each final $s_i^{n_i}$ [13], e.g., $\bar{B} \rightarrow D$ and $\bar{B} \rightarrow D^*$, with $s_i^{n_i} = \frac{1}{2}^-$, are governed by a single function ξ , while transitions to the first $s_i^{n_i} = \frac{1}{2}^+$ and $s_i^{n_i} = \frac{3}{2}^+$ multiplets depend on functions called $\tau_{\frac{1}{2}}$ and $\tau_{\frac{3}{2}}$, respectively [14]. These latter decays to the $s_i^{n_i} = \frac{1}{2}^+$ and $s_i^{n_i} = \frac{3}{2}^+$ states, about 500 MeV above the ground states, are of particular interest: they are the most likely source of any discrepancy between the inclusive semileptonic rate and the sum over the D and D^* exclusive rates, and in addition the functions $\tau_{\frac{1}{2}}$ and $\tau_{\frac{3}{2}}$ are implicated in a Bjorken sum rule [15] for the slope near zero recoil of the function ξ .

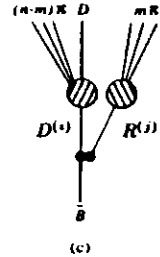
Fig. 1:



(a) A graphical representation of the "naive" factorization hypothesis for $B \rightarrow D + n\pi$, in which $B \rightarrow D + (n-m)\pi$ via the $\bar{c}\gamma^\nu(1-\gamma_5)b$ current and the $\bar{d}\gamma_\nu(1-\gamma_5)u$ current produces $m\pi$.



(b) The charm resonance dominance model of (a). Here $D^{(*)}$ is any charmed meson resonance, including the special case $D^{(*)} = D^*$. (Note also that the hatched circle includes the possible decay chain $D^{(*)} \rightarrow D^* + (n-m-1)\pi$.)



(c) Fig. 1(b) with the additional assumption that $m\pi$ production is resonant. Here $R^{(*)}$ is a resonance with π , ρ , or a_1 quantum numbers.

II. Factorization

A. Background

In the absence of strong interactions and for momentum transfers small with respect to M_W , the hadronic weak interaction responsible for $\bar{B} \rightarrow D + n\pi$ would have the naive current-current form

$$H_W = \frac{G_F}{\sqrt{2}} U_{ud}^* U_{cb} [\bar{c}\gamma^\nu(1-\gamma_5)b] [\bar{d}\gamma_\nu(1-\gamma_5)u]. \quad (1)$$

Strong interactions significantly modify this form, though their effect is only known analytically at short distances. If we renormalize our calculation at some scale μ with $\Lambda_{QCD} \ll \mu \ll M_W$, then the effective weak interaction due to graphs like those of Figure 2 at mass scales greater than μ is, in the leading logarithmic approximation [16],

$$H_W(\mu) = \frac{G_F}{\sqrt{2}} U_{ud}^* U_{cb} [c_1(\mu)h_1(\mu) + c_2(\mu)h_2(\mu)] \quad (2a)$$

where

$$h_1 = [\bar{c}\gamma^\nu(1-\gamma_5)b] [\bar{d}\gamma_\nu(1-\gamma_5)u] \quad (2b)$$

$$h_2 = [\bar{c}\gamma^\nu(1-\gamma_5)\frac{\lambda^i}{\sqrt{2}}b] [\bar{d}\gamma_\nu(1-\gamma_5)\frac{\lambda^i}{\sqrt{2}}u]. \quad (2c)$$

The λ^i are the Gell-Mann $SU(3)$ matrices so that h_2 is a singlet made of two currents which individually create states with octet quantum numbers. As discussed below, we will here choose $\mu = m_b$, in which case

$$c_1 = \frac{2}{3} \left[\frac{\alpha_s(m_W)}{\alpha_s(m_b)} \right]^{\frac{8}{3}} + \frac{1}{3} \left[\frac{\alpha_s(m_W)}{\alpha_s(m_b)} \right]^{-\frac{8}{3}} \quad (2d)$$

$$c_2 = \frac{1}{2} \left[\frac{\alpha_s(m_W)}{\alpha_s(m_b)} \right]^{\frac{8}{3}} - \frac{1}{2} \left[\frac{\alpha_s(m_W)}{\alpha_s(m_b)} \right]^{-\frac{8}{3}}. \quad (2e)$$

For future reference we note that (2d) and (2e) give $c_1 \simeq 1.03$ and $c_2 \simeq -0.26$.

While the form of expression (2) is natural (since in the absence of strong interactions $c_1 = 1$ and $c_2 = 0$) it is instructive to consider the alternative Fierz-transformed expression

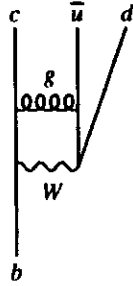


Fig. 2: A typical graph giving rise to the low-energy effective theory.

$$H_W(\mu) = \frac{G_F}{\sqrt{2}} U_{ud}^* U_{cs} [\tilde{c}_1(\mu) \tilde{h}_1(\mu) + \tilde{c}_0(\mu) \tilde{h}_0(\mu)] \quad (3a)$$

in which

$$\tilde{h}_1 = [d\gamma^\nu(1-\gamma_5)b] [\bar{c}\gamma_\nu(1-\gamma_5)u], \quad (3b)$$

$$\tilde{h}_0 = [d\gamma^\nu(1-\gamma_5)\frac{\lambda^i}{\sqrt{2}}b] [\bar{c}\gamma_\nu(1-\gamma_5)\frac{\lambda^i}{\sqrt{2}}u] \quad (3c)$$

with

$$\tilde{c}_1 = \frac{2}{3} \left[\frac{\alpha_s(m_W)}{\alpha_s(m_b)} \right]^{\frac{2}{3}} - \frac{1}{3} \left[\frac{\alpha_s(m_W)}{\alpha_s(m_b)} \right]^{-\frac{2}{3}} \quad (3d)$$

$$\tilde{c}_0 = \frac{1}{2} \left[\frac{\alpha_s(m_W)}{\alpha_s(m_b)} \right]^{\frac{2}{3}} + \frac{1}{2} \left[\frac{\alpha_s(m_W)}{\alpha_s(m_b)} \right]^{-\frac{2}{3}}. \quad (3e)$$

Note that $\tilde{c}_1 \simeq 0.11$ and $\tilde{c}_0 \simeq 1.12$, so that $3\tilde{c}_1^2 + \frac{2}{3}\tilde{c}_0^2 = 3\tilde{c}_1^2 + \frac{2}{3}\tilde{c}_0^2$ as required by duality (see below). This form shows that factorization has subtleties: the same interaction can be "factorized" in many different but equivalent ways.

In fact, the term "factorization" has been used to describe many different phenomenological hypotheses. The most extensively developed and widely discussed is that of Bauer, Stech, and Wirbel [4] (hereafter denoted BSW). In the general graph for the strong-interaction-dressed weak decay $\bar{B} \rightarrow D + \pi\pi$, the action of $H_W(\mu)$ not only destroys the b quark in \bar{B} , but also inserts the field operators \bar{c} , d , and u . These three operators can be arranged to be proportional to two different meson local interpolating field operators

$$d(x)\gamma_\nu(1-\gamma_5)u(x) \quad (4a)$$

and

$$\bar{c}(x)\gamma_\nu(1-\gamma_5)u(x) \quad (4b)$$

which appear in the forms of H_W given in Eqs. (2) and (3), respectively. The BSW phenomenology begins by re-expanding $H_W(\mu)$. Instead of expanding in terms of the

"orthogonal" operator pairs (h_1, h_8) and $(\tilde{h}_1, \tilde{h}_8)$ respectively, as in (2) and (3), they use the non-orthogonal operator basis (h_1, \tilde{h}_1) to obtain

$$H_W(\mu) = \frac{G_F}{\sqrt{2}} U_{ud}^* U_{cb} [\alpha_1(\mu) h_1(\mu) + \tilde{\alpha}_1(\mu) \tilde{h}_1(\mu)] \quad (5a)$$

in which

$$\alpha_1 = \frac{1}{2} \left(\left[\frac{\alpha_s(m_W)}{\alpha_s(m_b)} \right]^{\frac{3}{2}} + \left[\frac{\alpha_s(m_W)}{\alpha_s(m_s)} \right]^{-\frac{3}{2}} \right) = \tilde{c}_8 \quad (5b)$$

$$\tilde{\alpha}_1 = \frac{1}{2} \left(\left[\frac{\alpha_s(m_W)}{\alpha_s(m_b)} \right]^{\frac{3}{2}} - \left[\frac{\alpha_s(m_W)}{\alpha_s(m_s)} \right]^{-\frac{3}{2}} \right) = c_8. \quad (5c)$$

For future reference we note that $\alpha_1 \simeq 1.12$ and $\tilde{\alpha}_1 \simeq -0.26$. In this form $H_W(\mu)$ contains the interpolating fields (4a) and (4b) explicitly. BSW then make a further transformation to an effective interaction at the hadronic level in which they write

$$H_W^{(had)} = \frac{G_F}{\sqrt{2}} U_{ud}^* U_{cb} [a_1 h_1^{(had)} + \tilde{a}_1 \tilde{h}_1^{(had)}], \quad (6a)$$

where $h_1^{(had)}$ and $\tilde{h}_1^{(had)}$ are now imagined to contain the hadronic asymptotic fields created by the interpolating operators (4a) and (4b) respectively (e.g., as a result $h_1^{(had)}$ contains the hadronic π^- interpolating field corresponding to (4a) produced by both h_1 and \tilde{h}_1 of Eq. (5a)). The basic factorization assumption of BSW is that these hadronic fields do not interact once they are created by $H_W^{(had)}$. In the case of $h_1^{(had)}$, the $\bar{d}(x)\gamma_\nu(1-\gamma_5)u(x)$ current creates an $m\pi$ state with the quantum numbers of the π^-, ρ^- , or the a_1^- , while the remaining particles required for the $\tilde{B} \rightarrow D^{(*)} + n^{(*)}\pi$ transition (here $D^{(*)}$ is D or D^* , corresponding to $n^{(*)} = n$ or $n-1$) are made by the $(D^{(*)} + (n^{(*)} - m)\pi[\bar{c}(x)\gamma_\nu(1-\gamma_5)b(x)]\tilde{B})$ current matrix element. In the case of \tilde{h}_1 , the $\bar{c}(x)\gamma_\nu(1-\gamma_5)u(x)$ current creates a $D^{(*)} + (n^{(*)} - \tilde{m})\pi$ state with the quantum numbers of the D^0, D^{*0}, D_s^{*0} , or D_1^0 , while the remaining $\tilde{m}\pi$ are made by the $(\tilde{m}\pi[\bar{d}(x)\gamma_\nu(1-\gamma_5)b(x)]\tilde{B})$ current matrix element.

Clearly, factorization will require very special circumstances. In general, the interactions in the low energy hadronic effective theory will lead to strong interactions of the state produced by the interpolating fields of Eqs. (4a) and (4b) with the other hadrons

created in the decay. It is also clear that in general these interactions will obscure the short distance radiative corrections embodied in the c_1 and \tilde{c}_1 coefficients: the final states produced by h_1 and \tilde{h}_1 can always scatter into one another by strong interactions. (For example, h_1 and \tilde{h}_1 can make $\tilde{B}^0 \rightarrow D^+ \pi^-$ and $D^0 \pi^0$ respectively, but $D^+ \pi^- \rightarrow D^0 \pi^0$ is an allowed strong charge exchange interaction.)

Without considering such complications, one might have expected based on (5) that

$$a_1 = \alpha_1 + \frac{1}{3}\tilde{\alpha}_1 = c_1 \quad (6b)$$

$$\tilde{a}_1 = \tilde{\alpha}_1 + \frac{1}{3}\alpha_1 = \tilde{c}_1, \quad (6c)$$

since under a (purely kinematical) Fierz rearrangement, \tilde{h}_1 contains with a coefficient $\frac{1}{N_c}$ the same color singlet interpolating operators as those appearing in h_1 . (Note that this is simply the observation that, in Eqs. (2) and (3), only the h_1 and \tilde{h}_1 pieces, respectively, are active; see Appendix A for an interpretation of the color octet states.) However, fits to the analogous D -meson decays rule out this simple version of the factorization hypothesis (if one assumes its validity for the decay of the c quark). BSW therefore make the conservative and, as just discussed, well-motivated [17] generalization of allowing a_1 and \tilde{a}_1 to be free parameters. This procedure has been remarkably successful. A very intriguing aspect of the resulting phenomenology, which has been emphasized by BSW and by Shifman [2], is that it favors $a_1 = \alpha_1$ and $\tilde{a}_1 = \tilde{\alpha}_1$. From (6b) and (6c) we see that this is suggestive of a $\frac{1}{N_c}$ expansion, but it remains unclear how discarding these particular $\frac{1}{N_c}$ terms can be justified.

The preceding discussion will have made it clear that factorization, however defined, cannot hold in all circumstances. However, there are a variety of ways in which it could be true in certain special cases. As mentioned previously, it is possible that factorization could arise at high energy from color transparency [6]. Color transparency [18] is based on the observation that a pointlike color singlet state has no strong interactions. Since the interpolating fields (4a) and (4b) produce a virtual pointlike configuration, and since at high energy this state could propagate coherently out of the decay region, transparency

provides a possible mechanism for avoiding strong interactions that would ruin factorization. The $1/N_c$ limit [19] provides another possible argument for factorization [7]. In this limit mesons become narrow, non-interacting hadrons, and factorization follows.

Dugan and Grinstein [8] have used heavy quark effective theory [11] to provide a third possible scenario for factorization. The idea here is similar to that of transparency, but their approach indicates that factorization will hold in a much more restrictive kinematic regime than expected from either transparency or large N_c arguments: in this case factorization is expected only for heavy \rightarrow heavy-plus-light transitions in which the light quarks made by the (factorized) current are collinear and at high energy. In contrast, one would not expect factorization to hold for processes like $\bar{B} \rightarrow \pi\pi$ or $\bar{B} \rightarrow D\bar{D}_s$.

In Dugan-Grinstein factorization, a process like $\bar{B} \rightarrow D\pi$ proceeds only through h_1 : h_2 decouples in the kinematic regime considered. Moreover, Dugan and Grinstein point out that the resulting suppression by $\sqrt{q^2}$ (where q^2 is the squared invariant mass of the $\bar{u}d$ hadronic system and $E = \frac{(m_b^2 - m_c^2)}{2m_b}$) of the c_0 contribution to the \tilde{h}_1 term ($\tilde{c}_1 = \frac{2}{3}c_0 + \frac{1}{3}c_1$) is consistent with the expected suppression of the c_1 contribution to this term. The reason for this latter suppression is simple and can help us to understand the mechanisms underlying the suppression of h_1 (as we will see below). The h_1 interaction makes a $\bar{B} \rightarrow D^{(i)}$ -type transition via a form factor and the purely light hadronic system by a hard current, while \tilde{h}_1 makes the light system via a $\bar{B} \rightarrow$ light form factor. The latter will always be much softer since in the $\bar{B} \rightarrow D^{(i)}$ transition the heavy c -quark obtains most of the momentum of the $D^{(i)}$ directly from the hard $b \rightarrow c$ current. Dugan and Grinstein argue, moreover, that as $m_b \rightarrow \infty$ the \tilde{h}_1 -induced contributions are of the same order (i.e., suppressed by a power of $\sqrt{q^2}$) as other non-leading contributions to the dominant (h_1 -induced) amplitude. This argument seems to us to have applicability outside the framework of Ref. [8]. Transparency-based arguments, for example, also require large relative momenta between the hadrons produced by the two currents which will simultaneously make the \tilde{h}_1 form factor small. Naively, at least, one is led once again to the conclusion that corrections to the h_1 amplitude may be of the same order as the \tilde{h}_1 amplitude. Large N_c arguments do not require large momenta and accordingly predict a very different pattern of corrections to factorization. They nevertheless seem susceptible to an analogous objection. As

$1/N_c \rightarrow \infty$, there would be no corrections to the factorized transition amplitudes generated by h_1 and \tilde{h}_1 . However, in this limit the short-distance corrections also vanish, i.e. $c_1 = 1$ and $c_0 = 0$. Thus, both c_0 and corrections to factorization are $1/N_c$ effects [20]. (Although in the case of c_0 the coefficient of $1/N_c$ is $[\frac{2}{3}\frac{m_b}{m_c}]$, in practice this factor is not large compared to N_c .) Once again, the "factorisation limit" appears to involve only h_1 , with \tilde{h}_1 and corrections to h_1 arising as "non-leading" contributions.

We conclude that, at the moment at least, Dugan-Grinstein factorization offers the best hope of a systematic approach to weak hadronic decays, and we have therefore focused our efforts on testing and using this factorization hypothesis. (Other types of factorization can be tested using the methods we develop here, and we will comment on such extensions below.) It should be emphasized that Dugan-Grinstein factorization is very limited in its range of applicability. Imagine the Dalitz plot in the (E_d, q^2) plane for free $b \rightarrow cd\bar{u}$ decay based on the QCD-corrected interaction (2). The h_1 term will generate a $\bar{u}d$ system with q^2 from m_d^2 up to $q_{max}^2 \equiv (m_B - m_D)^2 \simeq 12 \text{ GeV}^2$. In the low mass region the $\bar{u}d$ pair will be moving approximately collinearly, so that the conditions for Dugan-Grinstein factorization apply. Conversely, the high mass region of the Dalitz plot corresponds to kinematical configurations in which the \bar{u} and d recoil in opposite directions so that they would not apply. More generally, Dugan-Grinstein factorization would hold in the Dalitz plot in those regions where $\frac{2m_b}{m_b + m_c} \left| \frac{q^2}{q_{max}^2} \right|^{1/2}$ is small. This region covers an increasingly large mass range as $m_b, m_c \rightarrow \infty$, but in the case at hand, where $(q_{max}^2)^{1/2} \simeq 3.4 \text{ GeV}$, we will (as mentioned already) probably have to restrict ourselves to low mass states. This analysis also tells us that, if we restrict ourselves to $q^2 < m_d^2$, we will be seeing only a small fraction of the rate from the h_1 term. In units of the $\bar{B} \rightarrow X_c e \bar{\nu}_e$ rate, the total rate from the h_1 term should be about $3c_1^2$, but we will only pick up roughly $\frac{m_d^2}{(m_B - m_D)^2} \simeq \frac{1}{4}$ of the Dalitz plot and therefore of that rate with our restriction on q^2 .

A similar analysis applied to the h_2 term is also interesting. Dugan and Grinstein show that if the \bar{u} and d quarks produced by the octet current are collinear and at large momenta, they will factorize and therefore not contribute to the production of a $\bar{u}d$ color singlet state. On the other hand, we know from duality that h_2 will contribute $\frac{2}{3}c_0^2$ units of inclusive semileptonic rate within the same Dalitz plot, even though, according to the

decoupling arguments of Dugan and Grinstein, it will not contribute to the exclusive channels to which factorization applies. This apparent contradiction would be resolved if the $\bar{u}d$ octet system were to produce a jet-like final state along its direction of motion. (In large N_c , this state would be equivalent to a state in which the \bar{u} was in a color singlet state with the b and the d in a color singlet state with the spectator "antiquark" of the original \bar{B} meson. The high energy \bar{u} and d would in this limit each make an independent e^+e^- -like jet, while remaining at low relative invariant mass, even though *not part of the same hadron*. Such a jet-like final state would be allowed by the Dugan-Grinstein argument since it would contain low energy quarks. Of course, it would *a fortiori* also not populate the low mass exclusive channels to which Dugan-Grinstein factorisation applies.

Given this understanding, we will in the first place focus on predictions which follow from h_1 only. Later we will discuss \bar{h}_1 -induced amplitudes as a way of setting the scale for expected corrections to Dugan-Grinstein factorization. (We emphasise that \bar{h}_1 -induced amplitudes can only be expected to indicate the size of such corrections; many other corrections of the same general magnitude are also expected.)

B. Implementation

Whether factorization requires a large relative energy between clusters or not, in this limit the situation is, as we have just discussed, considerably simplified. Consider, as a concrete example, $\bar{B} \rightarrow D\pi$. The h_1 term in Eq. (2) produces amplitudes for the decays $B^0 \rightarrow D^+ \pi^-$ and $B^- \rightarrow D^0 \pi^-$ while the \bar{h}_1 term in Eq. (3) produces amplitudes for $\bar{B}^0 \rightarrow \pi^0 D^0$ and $B^- \rightarrow \pi^- D^0$. In each case we have shown the final state with the hadron produced from the \bar{B} meson first and that from the currents of Eqs. (4) second to emphasize the important dynamical differences between these decays: in the heavy quark limit, the latter amplitudes will be of vanishing strength with respect to the former. As just discussed, this suppression occurs because the \bar{h}_1 amplitudes require that the d quark combine with the spectator light degrees of freedom in the \bar{B} to make the fast-moving pionic system, a process that will be strongly suppressed by a form factor since the momentum transfers to the light degrees of freedom are in the ratio $\tilde{Q}^2/Q^2 \sim m_D/m_1 \rightarrow \infty$, where m_1 is an effective mass for the light degrees of freedom. (See Ref. [21] for a discussion of

the behaviour of these form factors). Even without this dynamical suppression of the \bar{h}_1 term, its effect would still be small in \bar{B}^0 decays: the h_1 term leads in the general case to a negatively charged $m\pi$ system while \bar{h}_1 creates $(\bar{m}\pi)^0$. In the kinematic region of interest, these two processes don't interfere significantly. Thus the \bar{h}_1 contribution is suppressed relative to that of h_1 by a factor of $|\bar{c}_1/c_1|^2 \simeq 0.01$. On the other hand, in B^- decays both h_1 and \bar{h}_1 can lead to the same final state so there will generally be interference. In this case the importance of the \bar{h}_1 term is only diminished by \bar{c}_1/c_1 and the above-mentioned form factor suppression. This latter effect is the $\frac{\sqrt{s}}{E}$ -type suppression required by Dugan-Grinstein factorization. Note that with the neglect of \bar{h}_1 , some decays will be forbidden: e.g., in the example of $\bar{B} \rightarrow D\pi$, $\bar{B}^0 \rightarrow D^0 \pi^0$ will be forbidden.

In Dugan-Grinstein factorization, the restriction to high energy collinear quarks introduces additional anomalous scaling in the low energy effective weak interaction. For $m_b \geq E \gg m_c$, which is roughly the situation in nature, they find

$$\begin{aligned} \langle D^{(*)} + (\pi^{(*)} - m)\pi + m\pi | H_W^{eff}(\mu) | \bar{B} \rangle &= \frac{G_F}{\sqrt{2}} U_{cb}^* U_{cs} \left[\frac{\alpha_s(m_b)}{\alpha_s(E)} \right]^{-a_L} \left[\frac{\alpha_s(m_b)}{\alpha_s(m_c)} \right]^{a_L} \left[\frac{\alpha_s(m_c)}{\alpha_s(\mu)} \right]^{a_L} \\ &\times \left(\frac{2}{3} \left[\frac{\alpha_s(m_W)}{\alpha_s(m_b)} \right]^{\frac{2}{3}} \left[\frac{\alpha_s(m_b)}{\alpha_s(E)} \right]^{-\frac{2}{3}} + \frac{1}{3} \left[\frac{\alpha_s(m_W)}{\alpha_s(m_b)} \right]^{-\frac{2}{3}} \left[\frac{\alpha_s(m_b)}{\alpha_s(E)} \right]^{-\frac{2}{3}} \right) \\ &\times \langle D^{(*)} + (\pi^{(*)} - m)\pi | \mathbf{J}^\nu | \bar{B} \rangle \langle m\pi | \mathbf{j}_\nu | 0 \rangle \end{aligned} \quad (7a)$$

where \mathbf{J}^ν is the heavy quark current in the low energy heavy quark effective field theory [10,11], \mathbf{j}_ν is the light quark current in the Dugan-Grinstein "large energy effective theory",

$$a_L = -\frac{6}{25}, \quad (7b)$$

$$a_L = \frac{8}{27} \left[\frac{w \ln(w + \sqrt{w^2 - 1})}{\sqrt{w^2 - 1}} - 1 \right], \quad (7c)$$

and where α_s is the coupling appropriate to the theory with the number of active flavors in the interval over which the indicated leading logarithms are being summed. We have written (7a) in this peculiar form because in this kinematic situation $E \simeq \frac{1}{2}m_b$ so that $\frac{\alpha_s(m_b)}{\alpha_s(\bar{B})} \simeq 1$. If we make this approximation, then (7a) reduces to the scale-independent result

$$\langle D^{(*)} + (n^{(*)} - m)\pi + m\pi | H_W^{eff}(\mu) | \bar{B} \rangle = \frac{G_F}{\sqrt{2}} U_{cb}^* U_{cs} c_1 \langle D^{(*)} + (n^{(*)} - m)\pi | j^\nu | \bar{B} \rangle \langle m\pi | j_\nu | 0 \rangle \quad (8)$$

where the currents are now in the full theory since

$$\left[\frac{\alpha_s(m_b)}{\alpha_s(m_c)} \right]^{n_c} \left[\frac{\alpha_s(m_c)}{\alpha_s(\mu)} \right]^{n_L} \langle D^{(*)} + (n^{(*)} - m)\pi | j^\nu | \bar{B} \rangle$$

is the result of heavy quark effective field theory for the $\bar{B} \rightarrow D^{(*)} + (n^{(*)} - m)\pi$ matrix element. Since the D and D^* play a special role both experimentally and as members of the $s_7' = \frac{1}{2}^-$ heavy-quark-symmetry multiplet, we define

$$N^\nu(p, p', \{k_i\}, \lambda) = \langle D^{(*)}(p', \lambda), (n^{(*)} - m)\pi(\{k_i\}) | j^\nu | \bar{B}(p) \rangle \quad (9a)$$

$$M^\nu(q, \{k_i\}) = \langle m\pi(\{k_i\}) | j^\nu | 0 \rangle. \quad (9b)$$

Then, assuming factorisation and neglecting interference between processes with different m (see Ref. [22]), the contribution to the differential decay rate is

$$\frac{d\Gamma}{ds} = \frac{C \sqrt{(M_B^2 + M_D^2 - s)^2 - 4M_B^2 M_D^2}}{64\pi^2 M_B^2} \int \left(\prod_{i=1}^{n-m} \frac{d^3 k_i}{2E_{k_i} (2\pi)^3} \right) \sum_\lambda N^\nu N^{*\nu} \int d\Phi_{m\pi} M_\mu M_\mu^* \quad (10)$$

where $s = q^2$, $\Phi_{m\pi}$ is m -pion phase space for fixed q^μ , and $C = |G_F U_{cb}^* U_{cs}|^2$.

The decoupling of the heavy quark spin and flavor from the light degrees of freedom in interactions involving a single heavy quark generates relationships [10] among groups of current matrix elements, N^ν . In particular, all of the form factors for $\bar{B} \rightarrow D$ and $\bar{B} \rightarrow D^*$ are determined in the heavy quark limit in terms of a single function $\xi(w)$ of the scalar product $w = v \cdot v'$ of the four-velocities of the b and c quarks; moreover $\xi(1) = 1$. Other matrix elements involving a $b \rightarrow c$ transition can likewise be related using a small number of universal form factors. Here we will obtain the needed form factors from an empirical fit to the universal function $\xi(w)$ based on semileptonic decay data (see Fig. 3) along with the previously mentioned Bjorken sum rule. *Ultimately, these matrix elements N^ν can*

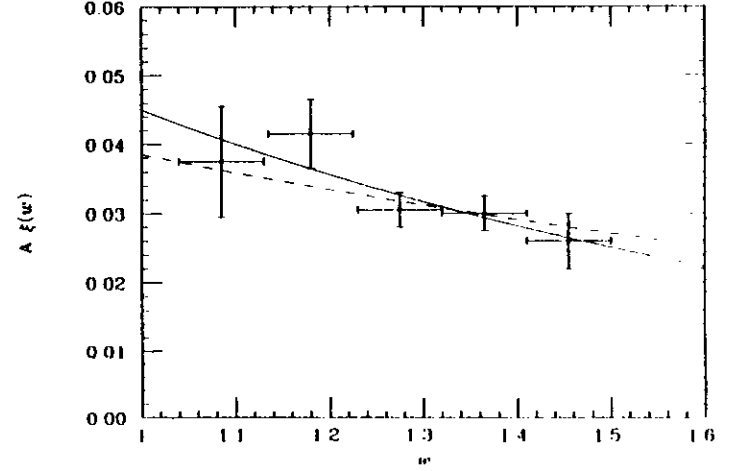


Fig. 3: A plot of $A\xi(w)$ versus w extracted from the combined CLEO and ARGUS $\bar{B}^0 \rightarrow D^* + \ell^- \bar{\nu}$ data [24] where $A = (\tau_B/1.18ps)^{1/2} |V_{cb}|$. The solid curve represents the best fit of $Ae^{\rho^2(w-1)}$. The dashed curve is constrained to $\rho^2 = 0.7$, from the model of Ref. [23].

all be extracted directly from semileptonic decays to provide a model-independent input to tests of factorization. Alternatively, if factorization is established in decays involving $\xi(\omega)$, it may prove to be more valuable to use hadronic weak \bar{B} decays to find excited D mesons and extract their universal form factors (e.g. the functions $\tau_{\frac{1}{2}}$ and $\tau_{\frac{3}{2}}$ mentioned previously) from non-leptonic data.

The m -pion phase space integral must have the form

$$\int d\Phi_{m\pi} M_\mu M_\nu^* = (q^\mu q^\nu - s g^{\mu\nu}) t_m(s) + q^\mu q^\nu l_m(s), \quad (11)$$

where the densities $t_m(s)$ and $l_m(s)$ can be extracted from $\tau \rightarrow \nu_\tau + m\pi$ angular distributions to provide the remaining model-independent input required to test factorization. The Appendix contains the formulae for $m \leq 3$. In fact, for $m = 3$ this relationship holds at the level of the three-pion Dalitz plot since the only available tensors that are rotationally invariant in their center of mass are $g^{\mu\nu}$ and $q^\mu q^\nu$, i.e.

$$\frac{d\Gamma}{ds_1 ds_2} = \frac{C \sqrt{(M_B^2 + M_D^2 - s)^2 - 4M_B^2 M_D^2}}{64\pi^2 M_B^3} \int \left(\prod_{i=1}^{(n-3)} \frac{d^3 k_i}{2E_{k_i}(2\pi)^3} \right) \sum_\lambda N^\mu N^{\nu*} \times \{ (q_\mu q_\nu - s g_{\mu\nu}) \tilde{t}_3(s, s_1, s_2) + q_\mu q_\nu \tilde{l}_3(s, s_1, s_2) \} \quad (12)$$

where $s_i = (q - k_i)^2$ and integrating $\tilde{t}_3(s, s_1, s_2)$ and $\tilde{l}_3(s, s_1, s_2)$ over the Dalitz plot region gives $t_3(s)$ and $l_3(s)$ respectively.

C. A Resonance Model for $\bar{B} \rightarrow D + n\pi$

As a prelude to the model-independent tests of factorization outlined above, we present here an initial calculation in which we assume resonance dominance of both current matrix elements. In the extreme and simplest version of this approximation, we assume that $\bar{B} \rightarrow D^{(*)} + n^{(*)}\pi$ proceeds via $\bar{B} \rightarrow D^{(*)}$ and vacuum $\rightarrow R^{(j)}$ where $D^{(*)}$ and $R^{(j)}$ are, respectively, charmed and uncharmed resonances treated in the narrow width approximation. Then the decays are all of the two-body type $\bar{B} \rightarrow D^{(*)} R^{(j)}$ (see Fig. 1(c)). The rate formulae for what should, in this limit, be an essentially exhaustive set of final states are given in Table 1. (The decay constants and form factors appearing in the Table are defined below).

General considerations suggest that the narrow resonance approximation will give a reasonably accurate picture of the rates to the channels of Table 1 in all cases except where $R^{(j)}$ is the a_1 ; in the numerical results shown in Table 2 we have accordingly taken the full three pion spectrum arising from the a_1 into account. On the other hand, we estimate that neglecting interference effects as in the narrow resonance approximation is reasonably accurate.

The results of Table 2 are thus based on formulae like

$$\Gamma_{\bar{B} \rightarrow D^{(*)} + n^{(*)}\pi} = \sum_{m=1}^n \sum_{D^{(*)}} (\Gamma_{\bar{B} \rightarrow D^{(*)} + m\pi}) (B_{D^{(*)} \rightarrow D^{(*)} + (n^{(*)} - m)\pi}), \quad (13)$$

where $B_{D^{(*)} \rightarrow D^{(*)} + (n^{(*)} - m)\pi}$ is the indicated branching fraction, deduced from heavy-quark symmetry [13]. In this framework, the factorization criteria of reference [8] are met by all diagrams. In the table we consider contributions from transitions of the \bar{B} via the $\bar{c}\gamma^\mu(1 - \gamma_5)b$ current to the ground state $s_L^{*c} = \frac{1}{2}^-$ multiplet (consisting of the $D(1870)$ and $D^*(2010)$), the $s_L^{*c} = \frac{1}{2}^+$ multiplet (consisting of $D_2^*(2460)$ and $D_1(2420)$), and the hypothetical $s_L^{*c} = \frac{1}{2}^+$ multiplet expected at about 2400 MeV (consisting of $D_1(\sim 2400)$ and $D_0^*(\sim 2400)$). We parametrize the three universal functions appearing in the twenty form factors of the twelve matrix elements $\langle D^{(j)} | j^\mu | \bar{B} \rangle$ according to

$$\xi(\omega) = e^{-\rho^2(\omega-1)} \quad (14a)$$

$$\tau_{\frac{1}{2}}(\omega) = \tau_{\frac{3}{2}}(\omega) = \tau(1)\xi(\omega), \quad (14b)$$

since $\xi(1) = 1$ is known from heavy-quark symmetry alone, and the model of reference [23] suggests that $\tau_{1/2}$ and $\tau_{3/2}$ are equal and proportional to ξ . If the Bjorken sum rule is approximately saturated by the lowest $s_L^{*c} = \frac{1}{2}^+$ and $s_L^{*c} = \frac{1}{2}^+$ states then

$$-\frac{d\xi}{d\omega} \Big|_{\omega=1} \simeq \frac{1}{4} + 3[\tau(1)]^2. \quad (14c)$$

A fit to Figure 3 (taken from Ref. [24]) gives $\rho^2 = 1.18 \pm 0.50$; Eq. (14c) then gives $\tau(1) = 0.56 \pm 0.15$. Given the errors, another reasonable choice would be to use the value $\rho^2 = 0.7$ predicted by the model of reference [23] and the corresponding value of $\tau(1) = 0.4$ from the Bjorken sum rule. We present the results of both parameter sets.

decay	partial width in units of $K(r, w)$	partial width in units of $K(r, w)$ neglecting the π , ρ and a_1 masses.
$\bar{B} \rightarrow D\pi$	$f_\pi^2 [\xi(w)]^2 (1-r)^2 (w+1)^2$	$f_\pi^2 [\xi(w)]^2 (1-r)^2 (1+r)^4 / 4r^2$
$\bar{B} \rightarrow D^*\pi$	$f_\pi^2 [\xi(w)]^2 (1+r)^2 (w^2-1)$	$f_\pi^2 [\xi(w)]^2 (1-r)^2 (1+r)^4 / 4r^2$
$\bar{B} \rightarrow D_0^*(\sim 2400)\pi$	$4f_\pi^2 [\tau_{\frac{1}{2}}(w)]^2 (1+r)^2 (w-1)^2$	$f_\pi^2 [\tau_{\frac{1}{2}}(w)]^2 (1-r)^4 (1+r)^2 / r^2$
$\bar{B} \rightarrow D_1(\sim 2400)\pi$	$4f_\pi^2 [\tau_{\frac{1}{2}}(w)]^2 (1-r)^2 (w^2-1)$	$f_\pi^2 [\tau_{\frac{1}{2}}(w)]^2 (1-r)^4 (1+r)^2 / r^2$
$\bar{B} \rightarrow D_1(2420)\pi$	$2f_\pi^2 [\tau_{\frac{3}{2}}(w)]^2 (1-r)^2 (w+1)^2 (w^2-1)$	$f_\pi^2 [\tau_{\frac{3}{2}}(w)]^2 (1-r)^4 (1+r)^6 / 8r^4$
$\bar{B} \rightarrow D_2^*(2460)\pi$	$2f_\pi^2 [\tau_{\frac{3}{2}}(w)]^2 (1+r)^2 (w^2-1)^2$	$f_\pi^2 [\tau_{\frac{3}{2}}(w)]^2 (1-r)^4 (1+r)^6 / 8r^4$
$\bar{B} \rightarrow D\rho$	$f_\rho^2 [\xi(w)]^2 (1+r)^2 (w^2-1)$	$f_\rho^2 [\xi(w)]^2 (1-r)^2 (1+r)^4 / 4r^2$
$\bar{B} \rightarrow D^*\rho$	$f_\rho^2 [\xi(w)]^2 [(1-r)^2 (w+1)^2 + 2s_+]$	$f_\rho^2 [\xi(w)]^2 (1-r)^2 (1+r)^4 / 4r^2$
$\bar{B} \rightarrow D_0^*(\sim 2400)\rho$	$f_\rho^2 [\tau_{\frac{1}{2}}(w)]^2 (1-r)^2 (w^2-1)$	$f_\rho^2 [\tau_{\frac{1}{2}}(w)]^2 (1-r)^4 (1+r)^2 / 4r^2$
$\bar{B} \rightarrow D_1(\sim 2400)\rho$	$4f_\rho^2 [\tau_{\frac{1}{2}}(w)]^2 [(1+r)^2 (w-1)^2 + 2s_-]$	$f_\rho^2 [\tau_{\frac{1}{2}}(w)]^2 (1-r)^4 (1+r)^2 / r^2$
$\bar{B} \rightarrow D_1(2420)\rho$	$f_\rho^2 [\tau_{\frac{3}{2}}(w)]^2 [2(1+r)^2 (w^2-1)^2 + s_-]$	$f_\rho^2 [\tau_{\frac{3}{2}}(w)]^2 (1-r)^4 (1+r)^6 / 8r^4$
$\bar{B} \rightarrow D_2^*(2460)\rho$	$f_\rho^2 [\tau_{\frac{3}{2}}(w)]^2 [2(1-r)^2 (w+1)^2 (w^2-1) + 3(w+1)^2 s_-]$	$f_\rho^2 [\tau_{\frac{3}{2}}(w)]^2 (1-r)^4 (1+r)^6 / 8r^4$
$\bar{B} \rightarrow Da_1$	$f_{a_1}^2 [\xi(w)]^2 (1+r)^2 (w^2-1)$	$f_{a_1}^2 [\xi(w)]^2 (1-r)^2 (1+r)^4 / 4r^2$
$\bar{B} \rightarrow D^*a_1$	$f_{a_1}^2 [\xi(w)]^2 [(1-r)^2 (w+1)^2 + 2s_+]$	$f_{a_1}^2 [\xi(w)]^2 (1-r)^2 (1+r)^4 / 4r^2$

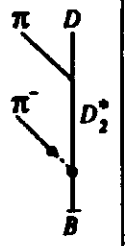
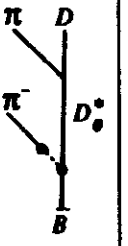
Table 1: Partial widths from h_1 only in the narrow width approximation.

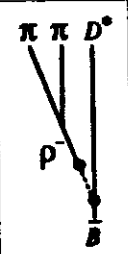
$K(r, w) = \frac{1}{16\pi} V_{ud}^2 V_{cb}^2 G_F^2 C_{cb}^2 c_1^2 M_B^3 r^2 \sqrt{w^2-1}$, $r = M_{D^{(i)}}/M_B$, $w = E_{D^{(i)}}/M_{D^{(i)}}$ and $s_\pm = (1+r^2-2rw)(w \pm 1 \mp \sqrt{w^2-1})^2$. Formulae for decays to any state with the quantum numbers of the π , ρ , or a_1 may be obtained by substitution of the appropriate coupling constant $f_{R^{(i)}}$. Similarly, formulae for decays to any state with the s_1^7 quantum numbers of the (D, D^*) , (D_1, D_2^*) , or (D_0^*, D_1) multiplets may be obtained by substitution of the appropriate universal form factors.

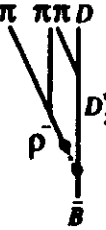
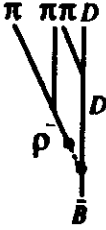
Table 2: The predictions of Dugan-Grinstein factorization expressed as a percentage of the $\bar{B} \rightarrow D^* e \bar{\nu}_e$ branching fraction. (For this we use the weighted average of the values quoted in Ref. [24], namely $4.4 \pm 0.6\%$.) The upper entries in the theoretical columns use $\rho^2 = 1.18$ and $\tau(1) = 0.56$, from a fit to Fig. 4, and the lower entries use $\rho^2 = 0.7$ and $\tau(1) = 0.4$, from the model of reference [23] and the Bjorken sum rule of Eq. (14c). The experimental results are, from top to bottom, CLEO 87, CLEO 85 and ARGUS [26]. Note that the $D + n\pi$ results *do not* include contributions from $D^* + (n - 1)\pi$. Here $D_1^{\frac{1}{2}}$ and $D_1^{\frac{3}{2}}$ represent the $D_1(\sim 2400)$ and $D_1(2420)$ respectively.

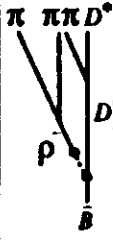
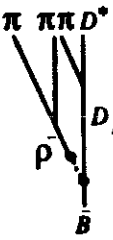
decay		experiment
$\bar{B}^0 \rightarrow D^+ \pi^-$	5.0	6.1 ± 2.0
	7.0	11.8 ± 7.1 10.9 ± 3.9
$\bar{B}^0 \rightarrow D^0 \pi^0$	0	-
	0	-
$B^- \rightarrow D^0 \pi^-$	5.0	11.4 ± 2.7
	7.0	12.5 ± 4.9 4.5 ± 2.4

decay		experiment
$\bar{B}^0 \rightarrow D^{*+} \pi^-$	5.6	9.1 ± 3.1
	7.2	6.6 ± 3.8 6.4 ± 2.6
$\bar{B}^0 \rightarrow D^{*0} \pi^0$	0	-
	0	-
$B^- \rightarrow D^{*0} \pi^-$	5.6	16.4 ± 5.9
	7.2	- 9.1 ± 4.4

decay		experimental $\bar{B} \rightarrow D\rho$		experimental via $D_2^*(2460)$		experimental via $D_0^*(\sim 2400)$	total	experiment
$\bar{B}^0 \rightarrow D^+ \pi^- \pi^0$	10.7	-	0.7	-	0.4	-	11.8	-
	14.5	20 ± 14	0.3	-	0.2	-	15.0	-
$\bar{B}^0 \rightarrow D^0 \pi^- \pi^+$	0	< 1.4	1.3	< 0.9	0.7	< 0.2	2.0	< 16
	0	-	0.7	-	0.4	-	1.1	-
$B^- \rightarrow D^0 \pi^- \pi^0$	10.7	-	0.7	-	0.4	-	11.8	-
	14.5	30 ± 14	0.3	-	0.2	-	15.0	-
$B^- \rightarrow D^+ \pi^- \pi^-$	0	-	1.3	< 9	0.7	< 11	2.0	< 16
	0	-	0.7	-	0.4	-	1.1	-

decay		experimental $\bar{B} \rightarrow D^* \rho$				total	experiment
$\bar{B}^0 \rightarrow D^{*+} \pi^- \pi^0$	12.6	43 ± 32	0.3	1.0	0.4	14.3	-
	15.9	16 ± 10	0.1	0.5	0.2	16.7	41 ± 15
$\bar{B}^0 \rightarrow D^{*0} \pi^- \pi^+$	0	-	0.5	1.9	0.7	3.1	-
	0	-	0.3	1.1	0.4	1.8	-
$B^- \rightarrow D^{*0} \pi^- \pi^0$	12.6	-	0.3	1.0	0.4	14.3	-
	15.9	23 ± 16	0.1	0.5	0.2	16.7	-
$B^- \rightarrow D^{*+} \pi^- \pi^-$	0	-	0.5	1.9	0.7	3.1	< 9
	0	-	0.3	1.1	0.4	1.8	5.5 ± 4.0 5.9 ± 3.7

decay		experiment via $\bar{B} \rightarrow D a_1$			experimental $\bar{B} \rightarrow D \rho \pi$ nonresonant	experimental $\bar{B} \rightarrow D \pi \pi \pi$ nonresonant	total	experiment
$\bar{B}^0 \rightarrow D^+ \pi^- \pi^0 \pi^0$	3.7	-	1.6	0.8	-	-	6.1	-
	4.9	-	0.8	0.4	-	-	6.1	-
$\bar{B}^0 \rightarrow D^+ \pi^- \pi^- \pi^+$	3.7	6.8 ± 3.8	0	0	2.5 ± 2.3	8.9 ± 7.1	3.7	18.2 ± 6.3
	4.9	-	0	0	-	-	4.9	-
$\bar{B}^0 \rightarrow D^0 \pi^0 \pi^- \pi^+$	0	-	3.2	1.5	-	-	4.7	-
	0	-	1.6	0.8	-	-	2.4	-
$B^- \rightarrow D^0 \pi^- \pi^0 \pi^0$	3.7	-	1.6	0.8	-	-	6.1	-
	4.9	-	0.8	0.4	-	-	6.1	-
$B^- \rightarrow D^0 \pi^- \pi^- \pi^+$	3.7	5.1 ± 4.2	0	0	9.5 ± 7.1	11.6 ± 9.5	3.7	26.1 ± 8.9
	4.9	-	0	0	-	-	4.9	-
$B^- \rightarrow D^+ \pi^0 \pi^- \pi^-$	0	-	3.2	1.5	-	-	4.7	-
	0	-	1.6	0.8	-	-	2.4	-

decay		exp. via $\bar{B} \rightarrow D^* a_1$				exp. $\bar{B} \rightarrow D^* \rho \pi$ nonres.	exp. $\bar{B} \rightarrow D^* \pi \pi \pi$ nonres.	total	exp.
$\bar{B}^0 \rightarrow D^{*+} \pi^- \pi^0 \pi^0$	6.0	-	0.7	1.9	0.9	-	-	9.5	-
	7.1	-	0.3	1.0	0.5	-	-	8.9	-
$\bar{B}^0 \rightarrow D^{*+} \pi^- \pi^- \pi^+$	6.0	20.5 ± 10.0	0	0	0	15.5 ± 9.0	0.0 ± 0.2	6.0	36.1 ± 11.7
	7.1	-	0	0	0	-	-	7.1	27 ± 12
$\bar{B}^0 \rightarrow D^{*0} \pi^0 \pi^- \pi^+$	0	-	1.3	3.8	1.8	-	-	6.9	-
	0	-	0.7	2.1	0.9	-	-	3.7	-
$B^- \rightarrow D^{*0} \pi^- \pi^0 \pi^0$	6.0	-	0.7	1.9	0.9	-	-	9.5	-
	7.1	-	0.3	1.0	0.5	-	-	8.9	-
$B^- \rightarrow D^{*0} \pi^- \pi^- \pi^+$	6.0	-	0	0	0	-	-	6.0	-
	7.1	-	0	0	0	-	-	7.1	-
$B^- \rightarrow D^{*+} \pi^- \pi^- \pi^0$	0	-	1.3	3.8	1.8	-	-	6.9	-
	0	-	0.7	2.1	0.9	-	-	3.7	41 ± 21

We next turn to the $m\pi$ matrix elements. We use the definitions

$$\langle \pi(q) | j^\mu(0) | 0 \rangle = -i f_\pi q^\mu \quad (15a)$$

$$\langle \rho(q, \lambda) | j^\mu(0) | 0 \rangle = M_\rho f_\rho \epsilon^{*\mu}(q, \lambda). \quad (15b)$$

$$\langle a_1(q, \lambda) | j^\mu(0) | 0 \rangle = M_{a_1} f_{a_1} \epsilon^{*\mu}(q, \lambda). \quad (15c)$$

and obtain the values $|f_\pi| = 0.132$ GeV and $M_\rho |f_\rho| = 0.147 \pm 0.005$ GeV² from $\pi \rightarrow \mu\nu_\mu$ and $\tau \rightarrow \rho\nu_\tau$, respectively. (Note that the value of $M_\rho |f_\rho| = 0.12 \pm 0.01$ GeV², from $\rho \rightarrow e^+e^-$ and $\mu^+\mu^-$ is in mild disagreement with value from τ decay.) For $m = 3$, we use the model of Ref. [25] which gives $m_{a_1} = 1220 \pm 15$ MeV, $\Gamma_{a_1} = 420 \pm 40$ MeV and $M_{a_1} |f_{a_1}| = 0.25 \pm 0.02$ GeV². The transverse spectral density $\tilde{i}_2(s, s_1, s_2)$ was taken to be the ρ_i of Ref. [25] while the longitudinal spectral density was ignored as only the $\pi(1300)$ and non-resonant background, both tiny, can contribute to it. This model gives an excellent fit to the experimental $\frac{d\Gamma_{\tau \rightarrow \nu_\tau \pi^+ \pi^-}}{ds}$ data and a good fit to the Dalitz plot projections. We have, in addition to the π' , also ignored the radial excitations of the ρ and a_1 as well as the ρ -like 3D_1 states. Fig. 4 shows the expected differential decay rate for the a_1 contribution to $\bar{B} \rightarrow D^{(*)} + 3\pi$.

Table 3 shows the contributions to departures from the pattern of Table 2 due to the \tilde{h}_1 -induced amplitudes using the model of Ref. [23] for the $\bar{B} \rightarrow R^{(j)}$ matrix elements. The calculation of the \tilde{h}_1 amplitudes also requires knowledge of f_D , the analogue of f_π , which is not yet known experimentally. The rates shown are based on the nominal value $f_D = 150$ MeV [27]. Table 3 indicates that the processes $\bar{B}^0 \rightarrow D^{(*)0} \pi^0$, $\bar{B}^0 \rightarrow D^{(*)0} \rho^0$, and $\bar{B}^0 \rightarrow D^{(*)0} a_1^0$ will provide good tests of factorization. These rates are predicted to be so small that it seems likely that these processes will actually occur by $D^{(*)+} R^- \rightarrow D^{(*)0} R^0$ rescattering, i.e. via a direct breakdown of the factorization hypothesis. A measurement (or limit) on them will therefore provide a good test of the validity of factorization. (In the BSW model, these processes would appear with rates proportional to $\tilde{a}_1^2 \gg \tilde{c}_1^2$. They are therefore especially good places to look for a breakdown of the BSW model. We reiterate that these rates are not quantitatively predicted by Dugan-Grinstein factorization; they are only predicted to be small with respect to h_1 -induced decays. Thus their observation at

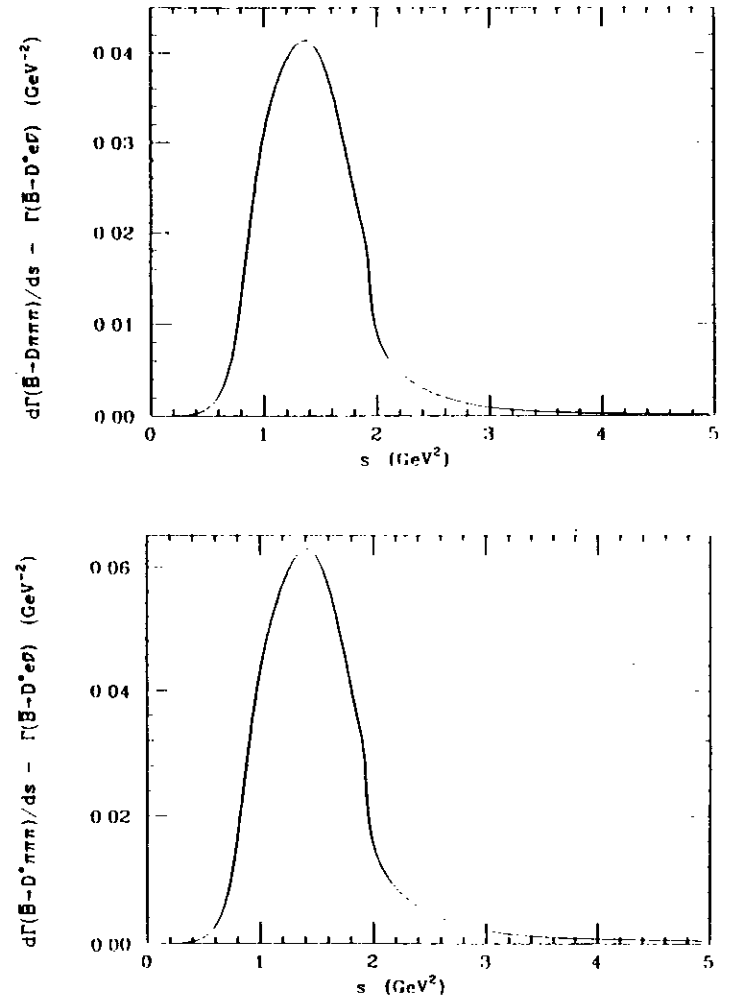


Fig. 4: The three pion spectrum predicted for the a_1 contribution to $\bar{B} \rightarrow D + 3\pi$ and $\bar{B} \rightarrow D^* + 3\pi$.

Table 3: An estimate of factorization-violating effects via \bar{h}_1 . We have ignored channels, other than $\bar{B}^0 \rightarrow D^{(*)0} \pi^0$, $\bar{B}^0 \rightarrow D^{(*)0} \rho^0$, and $\bar{B}^0 \rightarrow D^{(*)0} a_1^0$, with rates proportional to $|\bar{c}_1|^2 \simeq 0.01$; apart from these ignored channels, decays not listed here are unchanged from Table 2. As in Table 2, the upper entries have $\rho^3 = 1.18$ and the lower ones, $\rho^3 = 0.7$.

decay	$\Gamma/\Gamma_{B^0 \rightarrow D^{*0} \pi^0}$ (%) without \bar{h}_1	$\Gamma/\Gamma_{B^0 \rightarrow D^{*0} \pi^0}$ (%) with \bar{h}_1
$B^0 \rightarrow D^0 \pi^0$	0	0.006
	0	0.005
$B^0 \rightarrow D^{*0} \pi^0$	0	0.007
	0	0.006
$B^0 \rightarrow D^0 \rho^0$	0	0.007
	0	0.006
$\bar{B}^0 \rightarrow D^{*0} \rho^0$	0	0.021
	0	0.017
$B^0 \rightarrow D^0 a_1^0$	0	0.085
	0	0.068
$\bar{B}^0 \rightarrow D^{*0} a_1^0$	0	0.086
	0	0.061

decay	$\Gamma/\Gamma_{B^- \rightarrow D^{*0} \pi^-}$ (%) without \bar{h}_1	$\Gamma/\Gamma_{B^- \rightarrow D^{*0} \pi^-}$ (%) with \bar{h}_1
$B^- \rightarrow D^0 \pi^-$	5.0	5.6
	7.0	7.6
$B^- \rightarrow D^{*0} \pi^-$	5.6	5.1
	7.2	6.7
$B^- \rightarrow D^0 \pi^- \pi^0$	11.8	13.1
	15.0	16.3
$B^- \rightarrow D^0 \rho^-$	10.7	11.8
	14.5	15.6
$B^- \rightarrow D^+ \pi^- \pi^-$	2.0	2.6
	1.1	1.5
$B^- \rightarrow D^{*0} \pi^- \pi^0$	14.3	13.7
	16.7	16.0
$B^- \rightarrow D^{*0} \rho^-$	12.6	12.0
	15.9	15.2
$B^- \rightarrow D^{*+} \pi^- \pi^-$	3.1	3.1
	1.8	1.8
$B^- \rightarrow D^0 \pi^- \pi^0 \pi^0$	6.1	5.6
	6.1	5.5
$B^- \rightarrow D^0 \pi^+ \pi^- \pi^-$	3.7	3.0
	4.9	4.1
$B^- \rightarrow D^0 a_1^-$	7.4	5.9
	9.8	8.2
$B^- \rightarrow D^+ \pi^- \pi^- \pi^0$	4.7	5.3
	2.4	2.8
$B^- \rightarrow D^{*0} \pi^- \pi^0 \pi^0$	9.5	8.2
	8.9	7.3
$B^- \rightarrow D^{*0} \pi^+ \pi^- \pi^-$	6.0	4.7
	7.1	5.5
$B^- \rightarrow D^{*0} a_1^-$	12.0	9.4
	14.2	10.9
$B^- \rightarrow D^{*+} \pi^- \pi^- \pi^0$	6.9	7.0
	3.7	3.8

a small rate cannot be used to test Dugan-Grinstein factorization, but only to "calibrate" its accuracy. It should also be noted that our \tilde{h}_1 corrections tend to be much smaller and to have the opposite sign from those of the BSW model. This is because \tilde{a}_1/a_1 is substantial and negative, while \tilde{c}_1/c_1 is small and positive.)

III. Results

We now examine, in detail, the results displayed in Table 2:

1) $\tilde{B} \rightarrow D\pi$ and $\tilde{B} \rightarrow D^*\pi$

The decay $\tilde{B}^0 \rightarrow D^{(*)+}\pi^-$ is a pure \tilde{h}_1 decay, while $B^- \rightarrow D^{(*)0}\pi^-$ could have a factorization-violating \tilde{h}_1 amplitude which has been neglected in constructing Table 1. In the absence of \tilde{h}_1 , these pairs of rates would be identical and experiment is so far consistent with this simple picture. (Note that the BSW model predicts that $B^- \rightarrow D^{(*)0}\pi^-$ will be about 40% smaller than $B^0 \rightarrow D^{(*)+}\pi^-$.) This agreement provides support for both the factorization hypothesis and the predictions of heavy quark symmetry for the $\tilde{B} \rightarrow D$ and $\tilde{B} \rightarrow D^*$ matrix elements. It would obviously be desirable to measure the rates for $\tilde{B}^0 \rightarrow D^{(*)0}\pi^0$ which can proceed only via factorization-violating effects like \tilde{h}_1 and so are zero in the leading approximation (see Table 3).

2) $\tilde{B} \rightarrow D\pi\pi$ and $\tilde{B} \rightarrow D^*\pi\pi$

The rates for $\tilde{B} \rightarrow D\pi\pi$ are dominated by the process $\tilde{B} \rightarrow D\rho^-$ and $\tilde{B} \rightarrow D^*\pi^-$ with the former channel providing potential new tests of factorization (present data is not very stringent). In addition, the channels $\tilde{B}^0 \rightarrow D^0\pi^-\pi^+$ and $B^- \rightarrow D^+\pi^-\pi^-$ could be interesting since about 10% of these events are predicted to be due to decays of the $D_2^-(2460)$ and the hypothetical $D_2^0(\sim 2400)$. Such decays would of course be easily distinguished from the dominant $\tilde{B} \rightarrow D^*\pi^-$ mode.

The $\tilde{B}^0 \rightarrow D^0\pi^-\pi^+$ and $B^- \rightarrow D^+\pi^-\pi^-$ channels are even simpler: they are each predicted to occur only via the excited charmed $D_2^-(2460)$, $D_1(2420)$, and $D_1(\sim 2400)$ states. In addition, of course, $\tilde{B} \rightarrow D^*\rho$ provides further potential tests of factorization, and as already mentioned, the $D^{(*)}\rho^0$ channels may be especially revealing.

3) $\tilde{B} \rightarrow D\pi\pi\pi$ and $\tilde{B} \rightarrow D^*\pi\pi\pi$

These decays provide, in the first place, quantitatively new tests of factorization via $\tilde{B} \rightarrow D^{(*)}a_1^-$. The channels $\tilde{B}^0 \rightarrow D^+\pi^-\pi^-\pi^+$ and $B^- \rightarrow D^0\pi^-\pi^-\pi^+$ are particularly useful in this regard since they are free of the $D^*\rho$ channel. As mentioned earlier, the broad a_1 has some tactical advantages for testing Dugan-Grinstein factorization: it allows a test of factorization as a function of recoil momentum within a given channel since the 3π spectrum has significant strength from 0.5 GeV up to nearly 2 GeV. Four of the $\tilde{B} \rightarrow D^*\pi\pi\pi$ channels provide such tests.

The $\tilde{B} \rightarrow D^{(*)}\pi\pi\pi$ decays are also potentially rich sources of information on the excited D mesons, with significant contributions from both the $s_1^{\prime+} = \frac{1}{2}^+$ multiplet ($D_2^+(2460)$, $D_1(2420)$) and from the as yet unobserved $s_1^{\prime+} = \frac{1}{2}^+$ multiplet ($D_1(\sim 2400)$, $D_0^0(\sim 2400)$) expected nearby. The $\tilde{B} \rightarrow D^{(*)}\pi\pi\pi$ data also provide the strongest indication of significant departures from our calculation: the total rates for $\tilde{B} \rightarrow D^{(*)}\pi\pi\pi$ are predicted to be much smaller than the central values quoted by experiments (although the discrepancies are never much more than two standard deviations). Although it is possible, we would be surprised (see below) if the theoretical values were to change by factors of 2 as the result of the more rigorous, model-independent analysis we have outlined above. Moreover, since one of these decays is dominated by $D^*a_1^-$ and free of contributions from excited D mesons, the difficulty cannot be with our model for $\tau_{1/2}$ and $\tau_{3/2}$. Thus if these discrepancies persist, it is likely to signal a violation of the factorization hypothesis. It will also be interesting to see improved measurements of non- a_1 components to the decay $\tilde{B} \rightarrow D^{(*)}\rho^0\pi^-$. These processes are forbidden in the picture of Table 2. Finally, we note that the graphs of Fig. 4, showing the s -dependence of $\tilde{B} \rightarrow D + 3\pi$, could provide a further test of factorization. Any significant non-factorizing contributions obscured in the total width might be visible here. The shape of the experimental distribution could also provide clues regarding the source of the dominant corrections to the factorization approximation.

IV. Discussion

One of the least dependable elements of the calculations leading to Table 2 is our estimate of $\tau(1)$. Fortunately, at this stage the imprecision of our knowledge of $\tau(1)$ is not significant given the error limits of the present experimental data and the fact that most of the decays considered here are likely dominated by $\bar{B} \rightarrow D^{(*)}$ transitions.

Another concern is the possibility that we are neglecting important contributions to these decays with our assumption of resonance dominance. The historical success of this approach in similar situations make it unlikely that such contributions are very strong, but it will be interesting to check the data for such effects. (Note that $\bar{B} \rightarrow D^* + (3\pi)_{\text{nonresonant}}$ is already determined to be quite small.) The narrow resonance approximation itself should be satisfactory: most of the possible intermediate states are in fact narrow, while those that are broad do not seem capable of dramatically changing the results.

Both of the above reservations will be mitigated by improved semileptonic data. Given τ decay data, they are also the only significant sources of model dependence in our calculation that are relevant to the factorization issue since all that is required of the models for the amplitudes M^* is that they give the correct spectral densities, regardless of the veracity of the underlying physical picture.

In Table 3 we showed how the results of Table 2 would be modified by the simple addition of the \bar{h}_1 amplitudes for decays of particular interest. We note that \bar{h}_1 effects cannot be given with precision because of the large uncertainties that exist in the $\bar{B} \rightarrow$ light-hadron current matrix elements. We should also reemphasize that \bar{h}_1 effects by no means exhaust possible corrections to factorization; at best they may typify the size of corrections to be expected.

V. Conclusions

The preliminary results presented here are generally consistent with the factorization hypothesis. Taking the slightly preferred $\rho^2 = 0.7$ predictions as our benchmark, we find that all exclusive resonant rates are predicted correctly to within about 1.5 standard

deviations. For the total rates to the channels $D^{(*)} + n^{(*)}\pi$, this calculation fares less well: the central values predicted for $n^{(*)} \geq 2$ are all low by typically two standard deviations compared to the measurements which exist. Given this somewhat ominous indication, it is more important than ever to obtain completely model-independent predictions against which to test factorization, more precise experimental information on important modes, and stringent limits on (or observations of) modes forbidden in the "factorization limit".

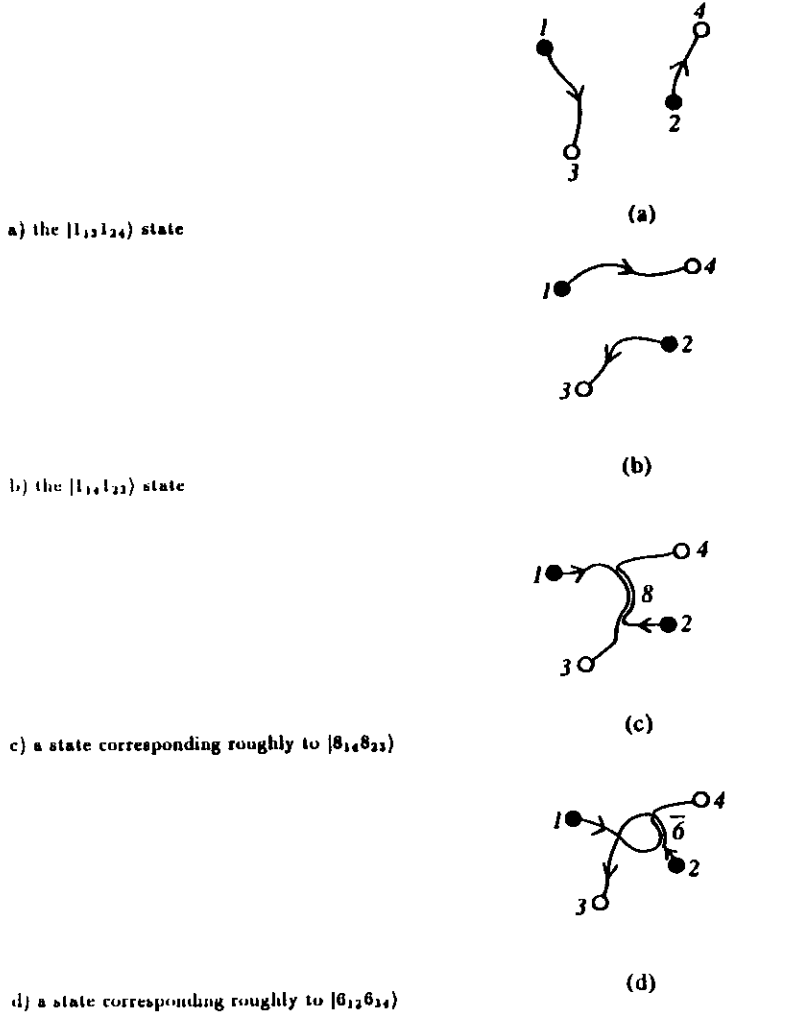
Appendix A: the h_8 and \bar{h}_8 interactions

In passing to the hadronic level in Eq. (6), the role of h_8 and \bar{h}_8 is obscure; here we will try to clarify the role of "octet states". In taking matrix elements of $H_W(\mu)$, we are making a transition from a quark-gluon basis for QCD at distances smaller than μ^{-1} to a hadronic basis for distances above this scale. This (nonrenormalisable) low energy effective theory contains all the meson states as "elementary" fields, and includes all possible couplings between these fields. When the local operator $H_W(\mu)$ acts, it produces (relative to the cutoff μ) a pointlike configuration of c , d , and \bar{u} quarks coupled to a color triplet (the state of the original b quark). As indicated by Eq. (2), such a state may be viewed as consisting of a linear combination of, e.g., a singlet π^- with a singlet D meson and an "octet π^- " with an "octet D meson". (The $\bar{c}(x)\gamma_\nu(1 - \gamma_5)d(x)$ current creates from the \bar{B} a singlet D meson if it is a color singlet current, and an "octet D meson" if it is an octet current). However, this does *not* mean that $H_W(\mu)$ produces new degrees of freedom, the so-called "hidden color states".

That the local $c\bar{d}\bar{u}$ state is produced in a color triplet state simply means that it is produced in a fixed (gauge invariant) linear combination of quark color states with respect to the color state of the annihilated b quark. The local $q\bar{q}$ bilinears in this linear combination then have amplitudes to produce mesons of the low energy effective theory out of vacuum. Configurations like $\pi_8 D_8$ do not correspond to new degrees of freedom, as evidenced by Eqs. (3c) and (3d) (see Fig. 5). Such states may, however, play a role in determining the *properties* (as opposed to the *degrees of freedom*) of the low energy effective theory. A local color singlet four quark operator like H_W contains only two linearly independent color configurations. These may be taken (in a self-explanatory notation) to be one of the orthogonal bases $\{|1_{13}1_{24}\rangle, |8_{13}8_{24}\rangle\}$, $\{|1_{14}1_{23}\rangle, |8_{14}8_{23}\rangle\}$, or $\{|\bar{3}_{12}3_{34}\rangle, |6_{12}\bar{6}_{34}\rangle\}$; alternatively, the two dimensional space could be spanned by the nonorthogonal basis $\{|1_{13}1_{24}\rangle, |1_{14}1_{23}\rangle\}$ (see Eqs. (5b) and (5c)). Thus configurations like $\pi_8 D_8$ have no dynamical significance locally. However, the *nonlocal* operator $\bar{\psi}_\delta(x_4)\psi_\beta(x_2)\bar{\psi}_\gamma(x_3)\psi_\alpha(x_1)$ is only locally color gauge invariant with the gluonic fields "excited" and these excitations can produce dynamical effects. This classification is easily seen in the lattice Hamiltonian strong coupling

basis (see the discussion in Ref. [28]) where a complete $q_1 q_2 \bar{q}_3 \bar{q}_4$ basis can be obtained from the (gauge invariant) nonlocal $|1_{13}1_{24}\rangle$ and $|1_{14}1_{23}\rangle$ states by coupling quarks to antiquarks, as indicated by the notation, with triplet link operators along arbitrary paths in the lattice. "Exotic" color states correspond in this basis to states where the link operators overlap (with each other or internally); see Fig. 5. When they overlap it can be convenient to re-expand the complete $\{|1_{13}1_{24}\rangle, |1_{14}1_{23}\rangle\}$ - type basis states on the multiply-excited links in terms of eigenstates of the $SU(3)$ Casimir. In Figs. 5(c) and 5(d) the $\mathbb{8}$ in $3 \times \bar{3}$ and the $\bar{\mathbb{6}}$ in 3×3 are shown.

Fig. 5: An illustration, in the flux tube model [28], of the completeness of the asymptotic meson states and the dynamical role of “exotic” color states.



Appendix B: the spectral densities l_m and l_n

For $m \leq 3$ the transverse and longitudinal densities of Section II. B can be extracted from τ decay data using the following expressions:

• the case $m = 1$:

This case is trivial as only $l_1(s)$ exists.

$$\frac{d\Gamma_{\tau \rightarrow \nu_\tau \pi}}{ds} = C_r l_1(m_\pi^2)(m_\tau^2 - m_\pi^2)^2 \quad (B1)$$

where $C_r = \frac{G_F^2 |V_{ud}|^2}{16 m_\tau \pi^2}$ and $l_1(s) = l_1(m_\pi^2) \delta(s - m_\pi^2)$.

• the case $m = 2$:

The decay distribution with respect to x_1 , the cosine of the polar angle of the π^- momentum where the z -axis is chosen along the direction of \vec{q} in the τ rest frame, can be used to find $l_2(s)$ and $t_2(s)$.

$$\frac{d\Gamma_{\tau \rightarrow \nu_\tau \pi \pi}}{ds dx_1} = \frac{C_r}{2} (m_\tau^2 - s)^2 \left[l_2(s) + \frac{3}{m_\tau^2} [(m_\tau^2 - s)x_1^2 + s] t_2(s) + 2\sqrt{3} x_1 \cos\phi \sqrt{l_2(s) t_2(s)} \right]. \quad (B2)$$

where the phase, ϕ , does not enter the calculation of B decay rates.

• the case $m = 3$:

In this case we use the distribution with respect to x_N , the cosine of the polar angle of the normal to the 3π decay plane in the rest frame of \vec{q} with the z -axis defined as above. At the level of the Dalitz plot, $\tilde{l}_3(s, s_1, s_2)$ and $\tilde{t}_3(s, s_1, s_2)$ can be extracted using

$$\frac{d\Gamma_{\tau \rightarrow \nu_\tau \pi \pi \pi}}{ds ds_1 ds_2 dx_N} = \frac{C_r}{2} (m_\tau^2 - s)^2 \left[\tilde{l}_3(s, s_1, s_2) + \frac{3}{2m_\tau^2} [(m_\tau^2 - s)(1 - x_N^2) + 2s] \tilde{t}_3(s, s_1, s_2) \right]. \quad (B3)$$

- 36**, 1289 (1987); CLEO Collaboration, D. Bortoletto *et al.*, *Phys. Rev. D* **45**, (1992).
- [27] For the $f_{D^{*1}}$ needed to construct Table 3 we use the non-relativistic quark model with harmonic oscillator wave functions, choosing the oscillator parameter to give reasonable agreement with known decay constants.
- [28] N. Isgur and J. Paton, *Phys. Lett.* **B124**, 247 (1983); *Phys. Rev. D* **31**, 2910 (1985).